

This item is the archived peer-reviewed author-version of:

New evidence on the origin of 'bee structures' on bitumen and oils, by atomic force microscopy (AFM) and confocal laser scanning microscopy (CLSM)

Reference:

Blom Johan, Soenen Hilde, Van den Brande Niko, Van den bergh Wim.- New evidence on the origin of 'bee structures' on bitumen and oils, by atomic force microscopy (AFM) and confocal laser scanning microscopy (CLSM)
Fuel - ISSN 1873-7153 - 303(2021), 121265
Full text (Publisher's DOI): <https://doi.org/10.1016/J.FUEL.2021.121265>
To cite this reference: <https://hdl.handle.net/10067/1793180151162165141>

New evidence on the origin of 'bee structures' on bitumen and oils, by atomic force microscopy (AFM) and confocal laser scanning microscopy (CLSM).

Abstract:

Microstructures on bitumen surfaces have been investigated extensively. Many studies have reported bee structures as well as other phases on bitumen surfaces. A lot of observations point into the direction of crystallisation of waxy compounds at least as an explanation for the bees. But there is still doubt about the origin of the other phases and the possible need for other bitumen components as promoters for the bee formation. In this study, bee structures are investigated by two microscopy techniques: atomic force microscopy (AFM) and confocal laser scanning microscopy (CLSM). By using wax model compounds, especially blends of waxes differing in melting points and chain lengths, bee structures and surrounding islands could be created on featureless bitumen surfaces. Structures very similar to what is observed on a paraffinic bitumen could be obtained. Moreover, bee structures could also be generated on other surfaces, such as mineral oil, and a maltene fraction. This indicates that bees are not restricted to bituminous materials and that bitumen components are not needed as promoters. Furthermore, CLSM offers possibilities to scan through transparent layers and to investigate surfaces under for example glass. In contact with such a solid substrate, as well as after water submersion, no microstructural features could be observed. Adding a combination of n-alkanes, to a transparent oil, displayed bees at the oil-air interface. The transparency of the oil allowed to investigate filler-oil interfaces created inside this sample. No bee structure could be detected at such interfaces.

Keywords; AFM, CLSM, mineral oil, bitumen, maltene, bees, wax

1. Introduction

The micromorphology of bituminous binders has been studied extensively [1-11], since Loeber reported atomic force microscopy (AFM) measurements in 1996. Typically, so-called bee structures, consisting of regular patterns of alternating hills and valleys, often in the shape of a bee, have been observed. Apart from bees, other phases have been identified, such as a peri-phase, which is solid-like and often forms a kind of shell around the bee phase, and a perpetua phase, which is softer or more viscous compared to the peri-phase and continuous in nature [4,13]. Most tests have been conducted on air-cooled surfaces, studies on fractured surfaces revealed no bees [12-14]. Parameters such as the sample preparation method, the thermal history and the change upon ageing and subsequent rejuvenation have been studied. For example, comparative studies of AFM and differentials scanning calorimetry (DSC) measurements have indicated that bees appear on binders containing crystallisable components. These bees disappear upon heating through a temperature range corresponding to endothermal transitions in DSC [16,17,19]. Furthermore, water exposure effects have been studied. Clear changes in the micromorphology and in bee patterns have been observed after leaving a bituminous surface in contact with water [20,21].

Most investigations have been based on AFM measurements. In an AFM microscope, a physical close or very near contact between the tip and the sample forms the basis for the measurement. To a certain extend other microscopy techniques have also been utilised [22-30], including optical dark [25, 26, 30]

and bright field microscopy [23], and scattering microscopy [27]. Non-contact methods have the advantage that they provide access to subsurface structures, provided the overlays are transparent. And as stated by Ramm et al. [26], they can characterise bitumen microstructures equally well at any temperature, whether the sample is frozen or heated beyond its melting point. Among other observations, Ramm et al. showed that bee structures do not form when the binder is covered with a glass slide, and that bee formation is reduced when binders are stored under for example glycerol [26]. These authors also noted subsurface microstructures of around $1 \mu\text{m}^2$, with no observable internal structure. Furthermore, time-of-flight secondary ion mass spectrometry (ToF-SIMS) measurements, which enable a chemical characterisation on a microscale level, have been applied [29]. These investigations concluded that aliphatic compounds are more represented in the bee structures compared to aromatic compounds.

Earlier investigations have shown that bee structures can be induced on a binder surface after adding waxy compounds. In this respect, waxes are defined as regular n-alkanes, or a blend of such alkanes, having the ability to crystallise [19,30-32]. These studies have provided further evidence that a crystallisation process is the starting point for the formation of bees. How such a crystallisation could evolve into a bee structure has been postulated by Lynn et al. [33]. These authors showed that the dimensions and the regularity of the patterns can be the result of wrinkling of the stiffer crystalline wax, floating on a less stiff bituminous surface. This was also confirmed by Hung et al. and Ramm et al. [21,25].

Although there is evidence that bee structures result from the crystallisation of waxes, there is still a debate whether all identified structures can be related to waxes. And, it is unclear whether asphaltenes or other bitumen components are necessary promoters for the bee formation [13,35-36]. Moreover, in literature, there is also an expectation that bee formation plays an essential role in the adhesion between a bituminous and a mineral surface, in dry and wet conditions.

In this research, the first aim is to present evidence that waxy components not only generate the bee structures but also other structures, which have been observed on bitumen. The second aim is to demonstrate that asphaltenes or other bituminous components do not take part in forming these bees. The third objective is to show that the medium in which the binders are stored strongly influences the formation or absence of bee structures. And finally, the last objective is to show that bees cannot be detected against a mineral surface.

The manuscript layout consists of three parts, as is schematically shown in figure 1. In the first part, two bituminous binders are investigated by two microscopy techniques, AFM and CLSM. One of the binders contained natural wax, while the second binder did not contain crystallisable components. Various n-alkanes were added to the non-waxy bitumen, and AFM and CLSM were applied to investigate the surface topographies. In a second part, the blend of n-alkanes, resulting in a clear bee structure on a bitumen surface, was added to the maltene fraction separated from the non-waxy binder and investigated by CLSM. The same procedure was performed for a standard mineral oil sample. And finally, in the last part, samples displaying bees on their air-cooled surfaces were investigated when brought into contact with a solid surface. Surfaces were also investigated after water exposure. And the mineral oil sample, as it was transparent, gave the possibility to be investigated not only at the oil-air surface but also deeper in the sample.

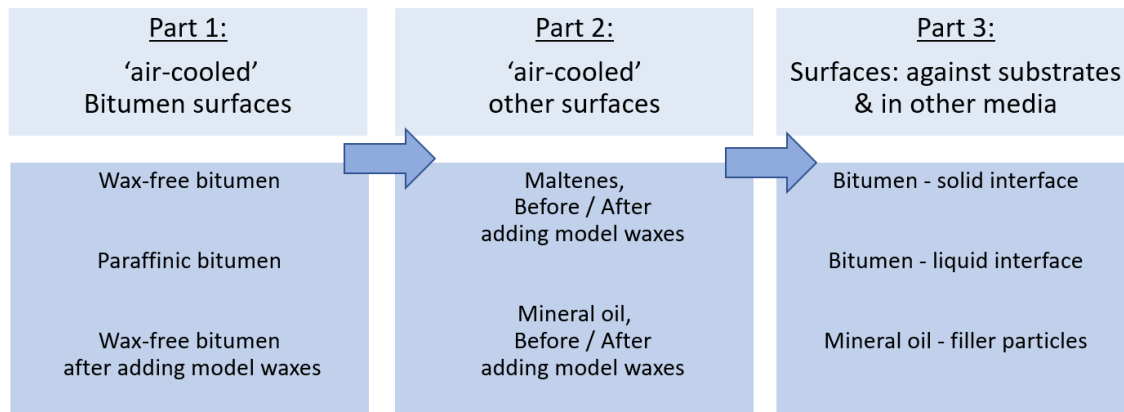


Figure 1: Schematic layout of the various parts of the paper.

2. Materials and techniques:

2.1. Materials:

An overview of the materials is provided in table 1. Two bitumen types were collected, from a naphthenic and a paraffinic crude source. The naphthenic bitumen was wax-free while the paraffinic bitumen contained wax, defined as crystallisable compounds. This was confirmed by DSC, these measurements are not included in this paper, but information on the testing can be found in ref. [17, 18, 24]. The complex viscosity, reported in table 1, was determined by a plate-plate rheometer at a frequency of 1 Hz, within the viscoelastic range. For the oil, the dynamic viscosity was determined in a rotational test within the Newtonian range. Furthermore, untreated glass slides (Menzel-Gläser, Thermo scientific) and a limestone filler (Duras 15), typical for asphalt construction, were used in the second and third part of the paper. The filler was derived from Sibelco, and according to their specifications, it consists 90 wt% of calcium carbonate, its density is between 2.6-2.8 g/cm³, and at least 74 wt% of all particles pass through a sieve of 0,063 mm, while 100 wt% through a sieve of 2 mm.

The two binders were investigated virgin and after a laboratory ageing cycle: The ageing consisted of a short-term ageing test, the rolling thin film over test (RTFOT), according to EN 12607. This short-term aging was followed by a long-term ageing test, based on the pressure ageing vessel (PAV), as described in EN 14769.

Table 1: Overview of the materials and some specifications.

| Description | Grade Type | Complex Viscosity (20°C, 1 Hz) Pa.s *Newtonian viscosity (20°C) Pa.s |
|--|------------|---|
| Naphthenic (wax-free) bitumen | 50/70 | 1.86E+06 |
| Paraffinic bitumen | 40/60 | 5.07E+06 |
| Maltene fraction separated from the wax-free bitumen by IP 143 | / | 1.48E+04 |
| Mineral oil: Castrol EDGE 5W-50 U.S | / | 0.279 * |

An overview of the model waxes is presented in table 2. The n-alkanes C18-C40 were acquired from TCI EUROPE NV, while the Sasobit was acquired from Sasol Performance Chemicals. The melting and boiling points of the n-alkanes are reported by TCI, the melting range of the Sasobit was recorded by DSC.

Table 2: Overview and physical properties of the waxes, added as model compounds.

| Code | Description | T-melting, °C | T-boiling, °C | purity |
|---------|--------------------------------|---------------|---------------|---------|
| C18 | n-alkane 18 carbons | 29 | 317 | > 98% |
| C24 | n-alkane 24 carbons | 52 | 391 | > 99.0% |
| C40 | n-alkane 40 carbons | 84 | 524 | > 97.0% |
| Sasobit | Fischer-Tropsch paraffine (FT) | 80-125 | - | - |

2.2. Samples with wax model compounds.

Bitumen and model waxes were blended, and each preparation consisted of 2 wt% of added wax relative to the total sample weight. Exact compositions are noted in the text. In some samples, only one type of n-alkane was added, while in other samples, a mixture of different waxes or n-alkanes was used.

Blends of bitumen and alkanes were prepared as follows: the bitumen was heated to 160 °C, an amount of binder was taken, left to cool to room temperature, and the desired amount of the respective n-alkane or FT paraffin was added. Afterwards, this blend was reheated to 160 °C for 30 minutes and homogenized by stirring the hot sample for at least 10 minutes. For the maltene and the oil sample, the same procedure was followed but, the homogenization temperature was reduced to 100°C.

2.3. Techniques.

In this research, an Asylum Research MFP-3D Atomic Force Microscope (AFM) was used. All AFM scans were performed using tapping mode in air and at 25 °C. Scanning was performed using an AC-160-TS silicon cantilever tip. The sample preparation is described below.

The Confocal Laser Scanning Microscope (CLSM) used in this study was a Keyence VK-X1000, with a VK-D1 motorised XY-stage, and with six objective lenses. The specifications, working distance and field of view of the lenses are shown in table 3. For the magnification of 50x, two lenses were available, a standard and a long distance lens. The magnification of the ocular was 24 and fixed. An electronic zoom up to eight times was also available. The lens with the highest magnification was a Nikon Lens Plan Apo EPI 150X, and according to specifications, it can acquire the surface profile with a vertical resolution of 5 nm and a lateral resolution of 10 nm.

Table 3: Specifications of the CLSM objective lenses

| Objective Lens | Working distance | Field of view (without/with XY-stage) |
|----------------|------------------|---------------------------------------|
| | mm | µm |
| 5 | 22.5 | 337 x 253 to 3699 x 2773 |
| 10 | 16.5 | 168 x 126 to 1849 x 1386 |
| 20 | 3.1 | 84 x 63 to 924 x 693 |
| 50 | 13.8 | 33.7 x 25.2 to 370 x 277 |
| 50 | 0.54 | 33.7 x 25.2 to 370 x 277 |
| 150 | 0.2 | 11 x 8.3 to 123 x 92 |

The CLSM uses two light sources: a laser light source, in this case with a wavelength of 661 nm, and a white light source. The laser information provides lateral resolution and measurement data, while the

white light source enables the capture of colour information, similar to an optical microscope. During the image scanning, focus variation was enabled. Focus variation allows capturing multiple images, while the lens moves up and down. These images are then used to construct a 3D shape according to the focus position.

The images obtained with the CLSM were post-processed by the VK Multi File Analyzer. Using the Differential Interference Contrast imaging method, nano-level features can be emphasised, resulting in 3D measurements. A specific advantage of the CLSM measuring sequence is that both optical and laser scanning “point cloud” information is stored. During processing high resolution images can be generated containing topological laser scanning information or real colour optical images or both.

Test specimen for AFM and CLSM measurements were prepared by first heating the binders to 160 C. After heating, a drop was applied to a glass slide. This slide was subsequently reheated to 140°C, on a hot stage for a few minutes, to spread the drop and to create a flat surface. Then, the samples were left to cool to room temperature. For the maltene and the oil sample, the procedure was the same, but the temperatures were reduced to 100°C, for both the homogenization and the further flattening of the drops. All measurements were conducted 24 hours after preparing the specimens.

3. Results:

3.1. Evaluation of air-cooled bitumen surfaces.

In figure 2, AFM and CLSM images of the two unmodified bituminous binders are represented. For the AFM tests, height and phase images are shown, for the CLSM 2D laser scanning images are included. For the virgin, paraffinic binder, the upper row in figure 2, bee structures are obvious, in AFM as well as in CLSM. In the AFM images, especially in the phase image, it is also clear that there is another phase surrounding each of the bees. This surrounding phase is not seen in the CLSM images. The observations are similar for the aged paraffinic binder, the second row in figure 2, but the bee structures are slightly longer in dimensions and fewer in number. Again, the islands surrounding the bees are obvious in the AFM phase image, but not seen in the CLSM. As expected, no structures were observed for the wax-free bitumen, not in AFM and not in CLSM. After ageing, this binder's images were the same as the ones before ageing, and therefore not added to figure 2.

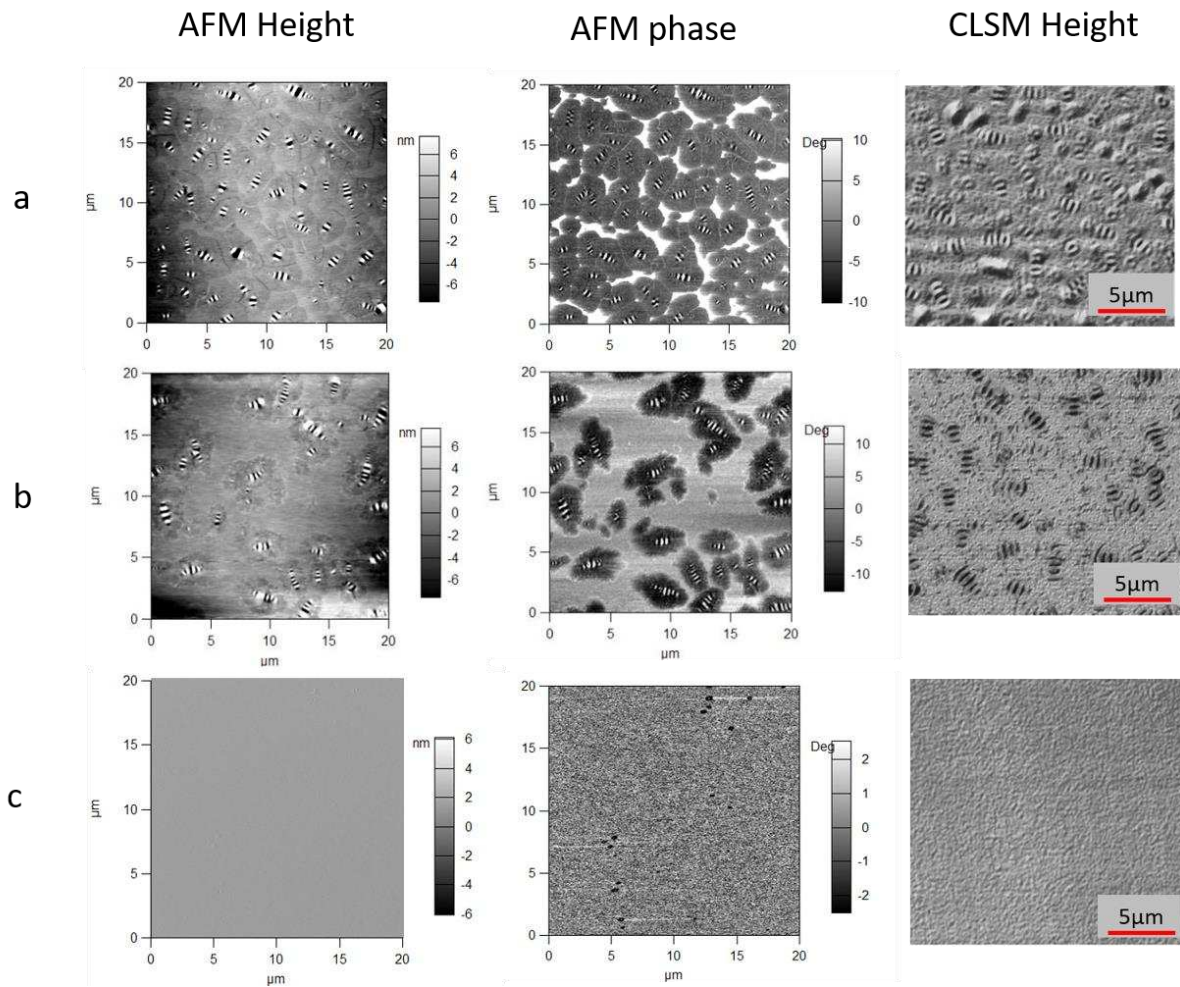


Figure 2: Air-cooled surfaces by AFM and CLSM: a) virgin paraffinic binder, b) aged paraffinic binder, c) virgin wax-free binder.

In figure 3, air-cooled surfaces of the wax-free binder after adding model waxes are illustrated. AFM and CLSM images are included. In figure 3a, 2 wt% C24 was added, and this does not induce bees under the conditions tested. Instead, it results in the formation of domains, as is shown in the AFM images. A clear effect is noted in the AFM phase image, and also in the AFM height image, a clear height difference can be observed. This will be discussed in more detail in figure 4. In the CLSM images of figure 3a, the left image represents the confocal optical and the right image the combined optical-laser, the same type of structure can also be observed.

Figure 3b & 3c refer to samples to which respectively 2 wt% C40 and 2 wt% Sasobit were added. The addition of the longer n-alkane C40, as well as the Sasobit induce bee structures, in the bitumen under investigation. And, it seems that when adding 2 wt% Sasobit, the observed bees are longer as for the sample containing 2 wt% of C40.

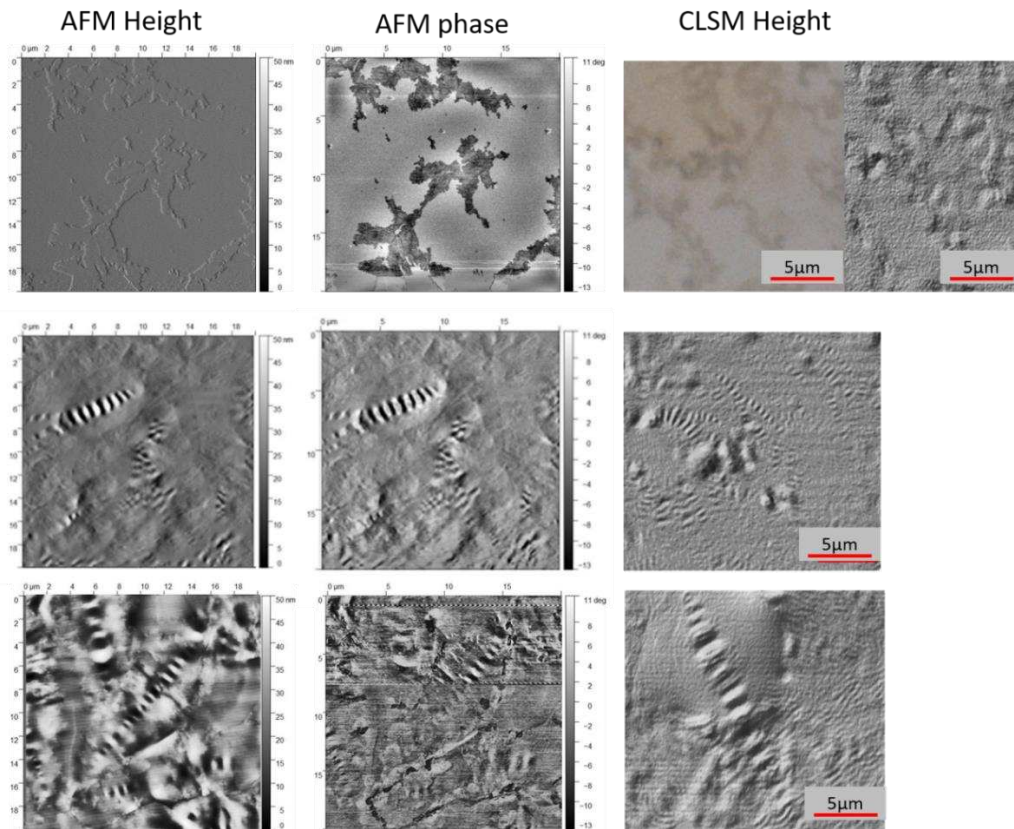


Figure 3: Air-cooled surfaces by AFM and CLSM of the wax-free binder after adding: a) 2 wt% C24, b) 2 wt% C40, c) 2 wt% Sasobit. For the image in case a) two images, an optical confocal scanning (left) and laser confocal scan (right) are included.

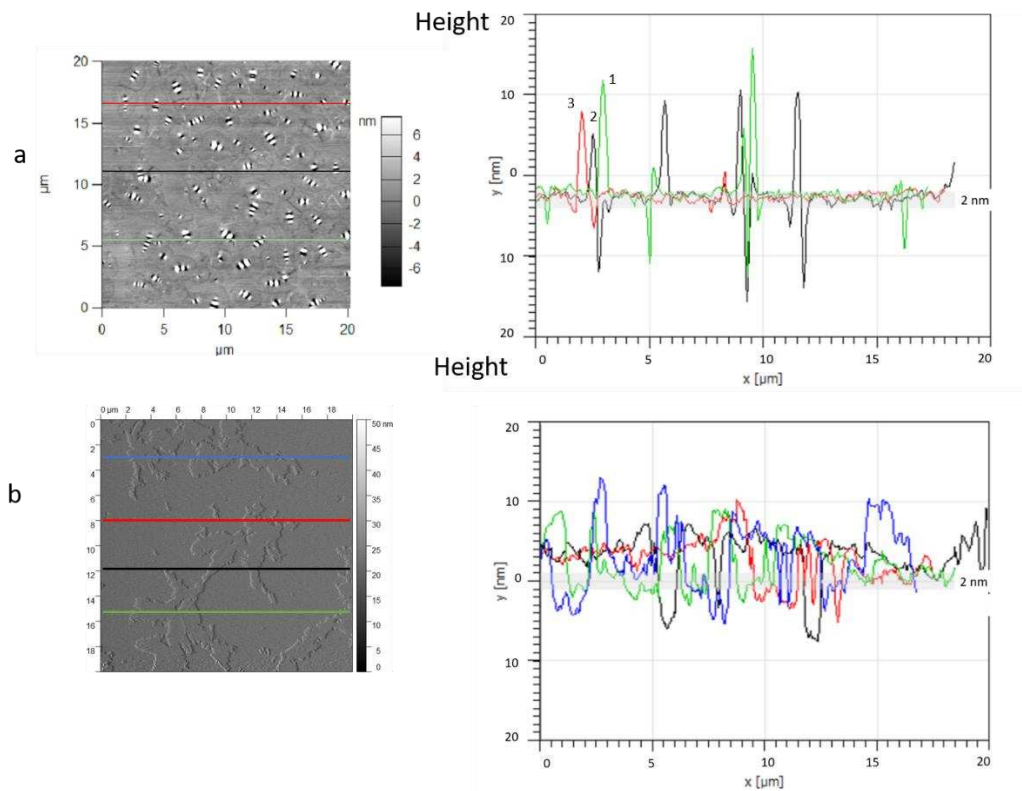


Figure 4: Representation of two height profiles, a: virgin paraffinic binder, b: wax free binder + 2 wt% C24

In figure 4, height profiles of two of the AFM images, shown before in figure 2a and 3a respectively, are plotted. Figure 4a, represents the profile of the virgin paraffinic binder, a sample that showed in the AFM test bee structures surrounded by small islands. The sharp signals in this height profile are related to the bees while the much smaller changes are due to the island phases. The four lines represent a profile scan at 4 different locations in the sample. These data indicate that the height difference associated with the AFM islands is very small, around and even below 2nm. As, this is below the vertical resolution of the CLSM, it is not observed in the corresponding CLSM images. Figure 4b represents the image of the wax-free binder after adding 2 wt% C24. This sample does not show bees, but it displays a two-phase structure. And the height profiles show a height variation of about 10 nm, a difference that can be captured by the CLSM. This explains why in the CLSM some height difference can be observed, while the islands surrounding the bees are typically not observed.

In figure 5, mixtures of two wax types were added to the wax-free binder, still keeping the total wax content at 2 wt%. Compared to figure 3a, where only one wax type was added, replacing a small amount of the 2 wt% C24 with the longer n-alkane C40, results in bee structure formation (figure 5a & b). The addition of a mixture of C18 and Sasobit, figure 5c, or the combination of the waxes with the lowest and highest melting temperatures, results in an image where bees are surrounded by small islands. This is very similar to what was observed for the paraffinic binder, shown in figure 2. Especially the image of the aged paraffinic binder, figure 2b, is almost the same as figure 5c. These images illustrate that by adding a mixture of wax compounds, the structures as observed on paraffinic binders can be generated in a wax-free binder. It also illustrates that not only the bees but also the islands can be generated.

Regarding the comparison of AFM and CLSM, the similarity between the height AFM and CLSM images is striking, bee structures are very similar for both measurements. However, the AFM phase images are not represented in the CLSM images, except if they are combined with a large enough height difference. In AFM tapping mode, an interaction between the tip and the surface is measured, allowing to record height patterns and changes in the tip's oscillation dampening, which is not possible in CLSM. This could indicate that the phase surrounding the bees, as in figure 2a and b, are more related to a change in harder and softer phases and have only a minor effect on the topography.

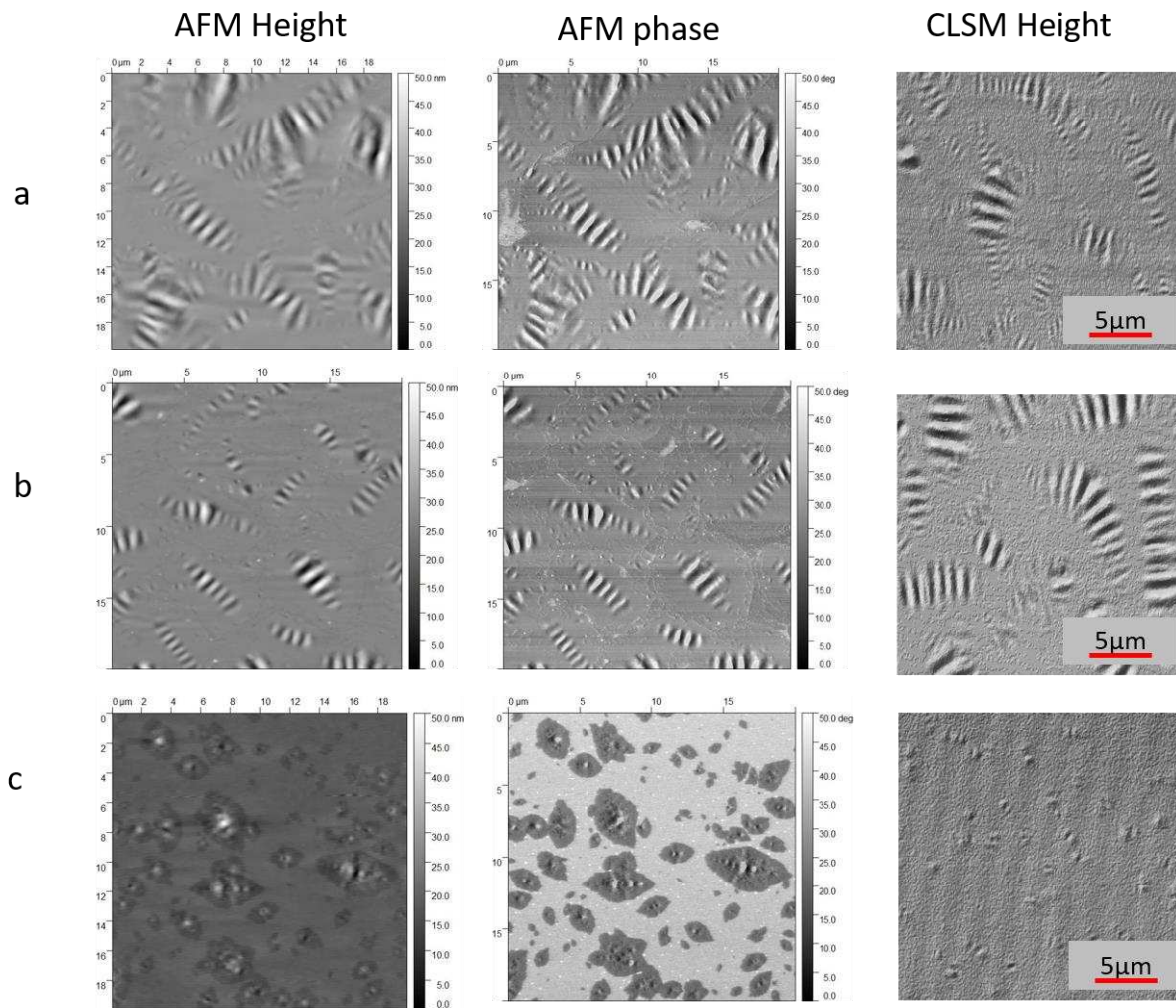


Figure 3: Air-cooled surfaces by AFM and CLSM of the wax-free bitumen after adding a mixture of various waxes: a) 1.5 wt% C24 + 0.5 wt% C40, b) 1.75 wt% C24 + 0.25 wt% C40, c) 1.75 wt% C24 + 0.25 wt% Sasobit

3.2. Evaluation of air-cooled surfaces of maltenes and oil.

The wax mixture of 1.75 wt% C24 + 0.25 wt% C40, as it induced a clear bee pattern in the wax-free bitumen, was selected as a modifier for other materials: a maltene and a mineral oil sample. Figure 6 shows CLSM images of air-cooled surfaces of the maltene sample, before and after adding this wax blend, respectively. The images clearly illustrate that bees are formed on a maltene surface, proving that asphaltenes are not needed to form this type of pattern.

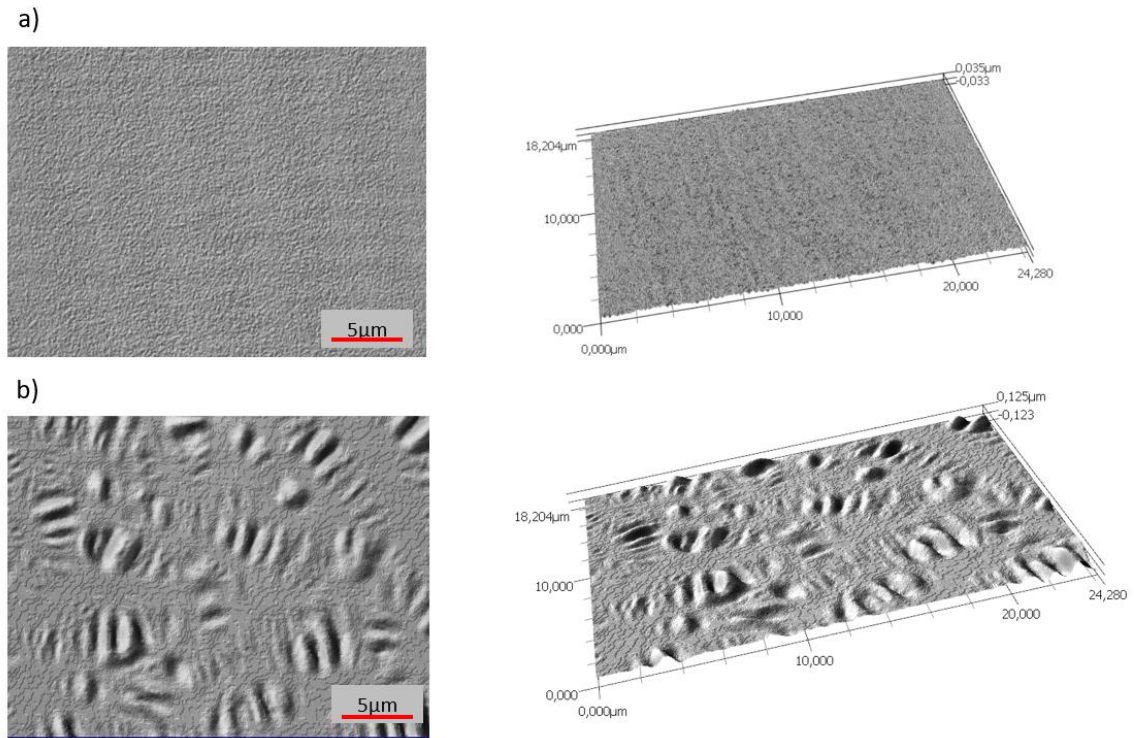


Figure 4: CLSM images of air-cooled surfaces of the maltene sample a) virgin sample, b) after adding 1.75 wt% C24 + 0.25 wt% C40.

In figure 7, the wax blend was mixed with the oil sample. Also, in this sample, it resulted in the formation of bee structures on the surface. This further demonstrates that bitumen components altogether are not needed to induce or promote bee formation. It also illustrates that CLSM is equally applicable to very hard as to very soft samples.

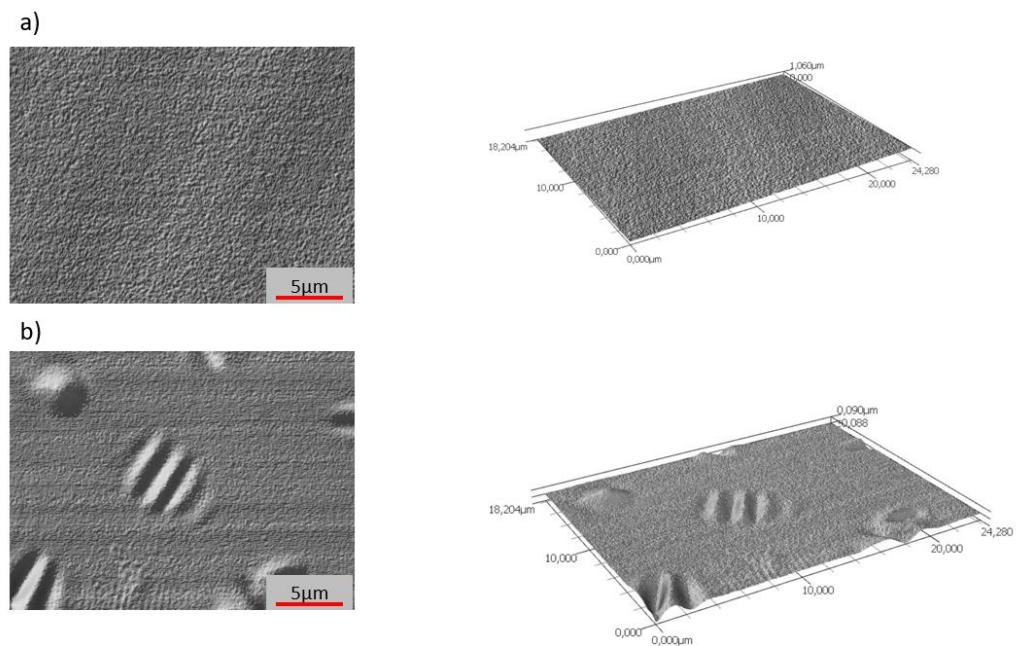


Figure 5: CLSM images of an air-cooled surface of: a) the virgin oil and b) the oil after adding 1.75 wt% C24 + 0.25 wt% C40.

3.3. The influence of substrate material.

In this section, the bitumen surface formed against a solid and a liquid substrate is investigated. The wax-free binder, after adding 1.75 wt% C24 + 0.25 wt% C40 was selected for these tests since it displays clear bees on its air-cooled surface, as shown in figure 5b. An untreated glass slide was chosen as the substrate. As it is transparent, it allows focusing the CLSM on the binder surface formed in contact with the substrate. In figure 8 surfaces in contact with glass, and the same surface in air are shown. On the air-bitumen surface, bees are clear, while at the bitumen-glass interface no bee structures can be found. These images show that bee structures are not formed under a solid substrate.

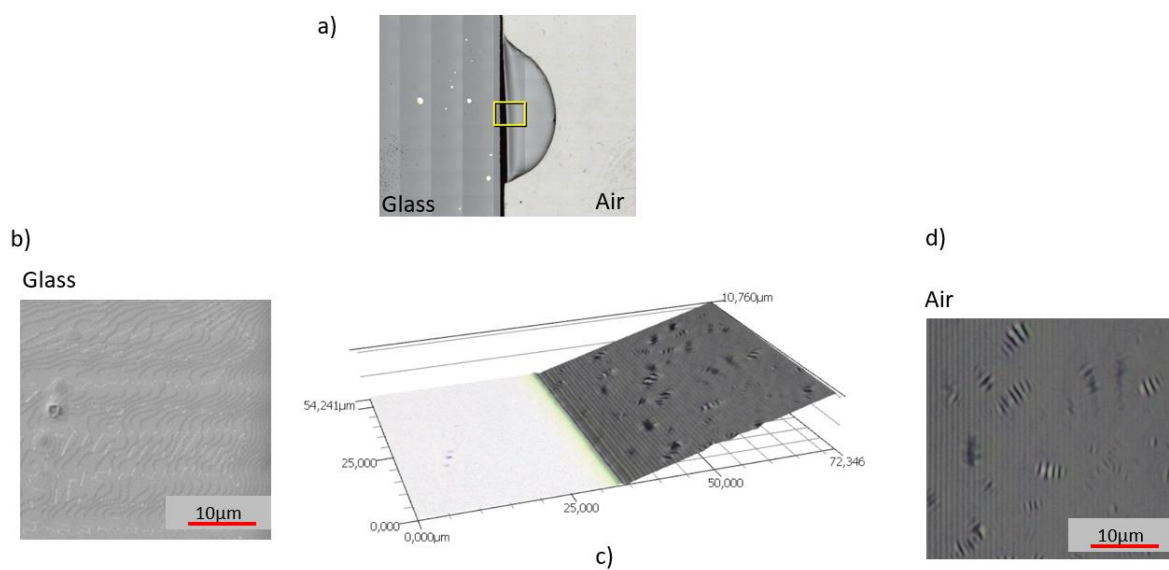


Figure 6: The wax-free binder, after adding 1.75 wt% C24 + 0.25 wt% C40 investigated at the bitumen-glass and at the bitumen-air interface: a) an overview of the sample, the yellow box indicates the position under investigation, b) image of the bitumen in contact with the glass surface, c) 3D image of the interface bitumen-glass and bitumen-air, the bitumen is the dark phase, d) the bitumen-air interface.

In figure 9, the wax-free binder's surface, after adding 1.75 wt% C24 + 0.25 wt% C40, was investigated under water. During the image recording, the water had to be removed; otherwise, undesired reflections appeared in the image. However, also, in this case, the binder surface does not show bee patterns. The small structures seen are due to the drying of the water before the measurement.

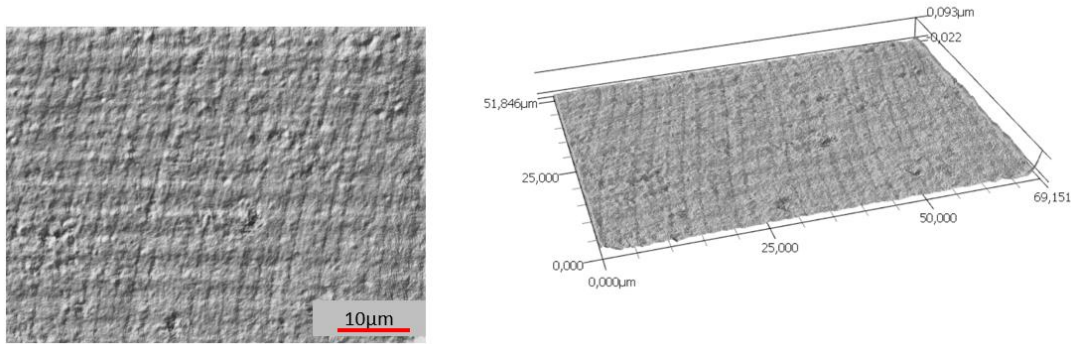


Figure 7: The wax-free binder, after adding 1.75 wt% C24 + 0.25 wt% C40 investigated under water.

The mineral oil sample, after adding the blend of waxes, 1.75 wt% C24 + 0.25 wt% C40, was investigated further. As shown before, this sample forms bee structures on the air-oil interface. And, as this oil is transparent, the CLSM can scan inside the bulk phase of the sample. For this purpose, the oil was placed in a cup, so that the sample thickness was about 3 mm. In a first experiment, the sample was investigated by CLSM below the surface, using the white light source. An image is shown in figure 10, this image shows a large number of particles between 5-10 microns. These particles were not observed in the virgin oil, so before the addition of the mixture of waxes. Therefore, the particles are also attributed to a wax crystallisation, taking place in the bulk of the sample. Similar experiments on bitumen or the maltene sample were not possible. These samples were not transparent enough to be investigated below the surface, with the current experimental setup.

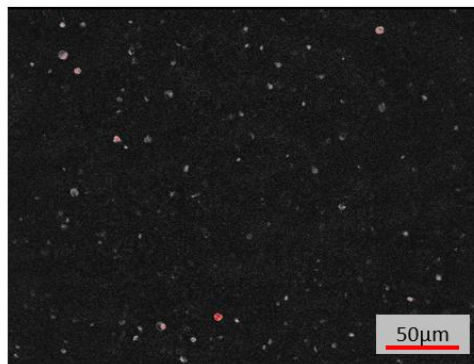


Figure 8: Confocal bright light image of the oil. The image is taken at 1 mm below the sample surface.

In a second experiment, 2 wt % of limestone filler particles were added to the oil-wax sample, and the sample was re-homogenised at 100 °C for 10 min and investigated after 24h dark storage at room temperature. In figure 11, microscopy images taken at three places in the sample are shown: a) at the air-oil surface, b) inside the oil sample and c) at the filler-oil interface. As expected, the air-oil interface shows bee patterns, while no such structures could be observed at the filler interface. This is in agreement with the observations at the binder-glass interfaces. It seems that bees are exclusively formed at the air-interface. It was again possible to take white light pictures inside the bulk sample,

which showed a similar image as already illustrated in figure10. The addition of the filler did not have an influence on the number and size of the particles.

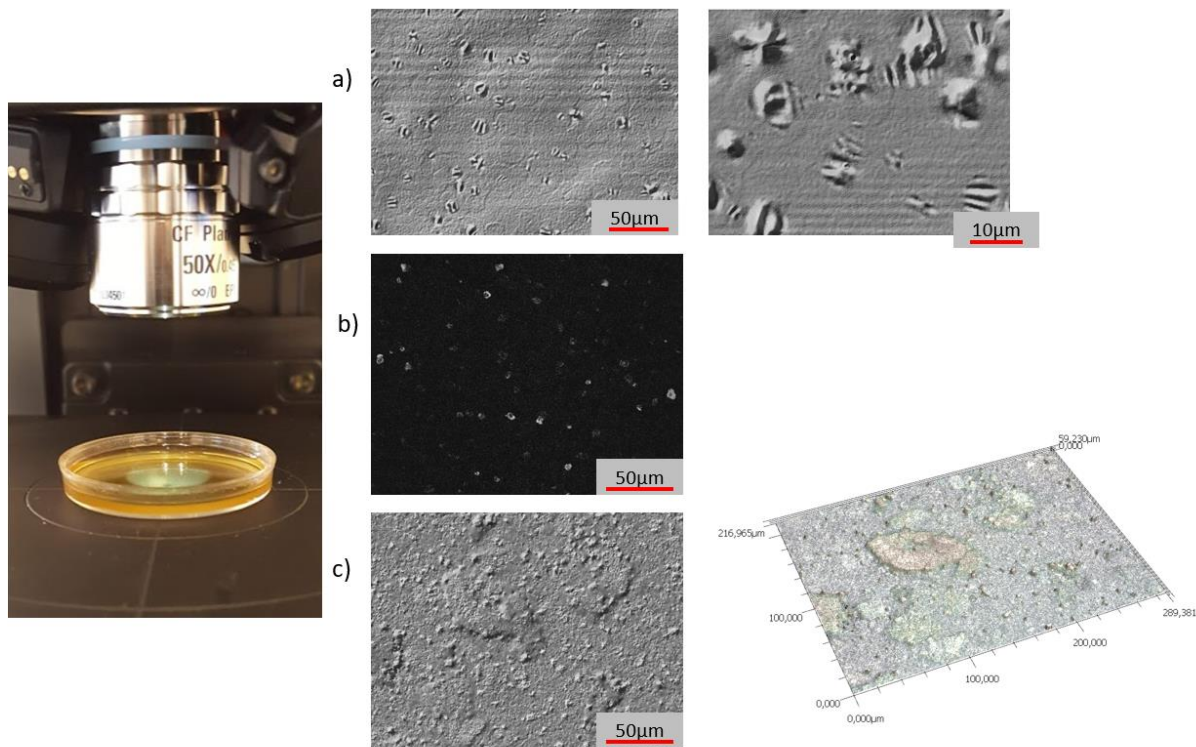


Figure 9: CLSM images of the oil with 1.75 wt% C24 + 0.25 wt% C40 with 2 wt% of filler: a) air-oil interface, b) bulk sample using white light, c) oil-filler interface.

4. Conclusions

Bee structures and the surrounding islands can be generated on binders that do not display any surface pattern, by adding model wax compounds. Depending on the type of waxes and the blend composition, different patterns can be obtained. An example is presented showing that the same structures observed on a paraffinic bitumen can be created by selecting the right combination of longer and shorter waxes. It is expected that this combination is bitumen specific.

Bee patterns are not limited to bituminous materials but can also be created on a mineral oil surface or bitumen fractions such as the maltene fraction. This proves that it is solely related to a crystallisation process of paraffins and that interference with or promotion by for example asphaltene or other bitumen components is not needed.

The studies with substrates demonstrate that bees are not formed on a bitumen-glass interface. Also, storage underwater entirely stops the bee formation. Moreover, by using transparent mineral oil to which a wax blend was added, it was possible to demonstrate that bees are not formed against a mineral surface, they were only observed at the oil-air interface. In the bulk of the modified oil, small particles were observed, and attributed to a wax crystallisation in the bulk phase.

The comparison of AFM and CLSM tests reveals that CLSM cannot observe changes in phase while AFM in tapping mode shows this in the phase image. On the other hand, as no contact is needed, CLSM can easily investigate hard, soft and liquid surfaces, and among other advantages, it allows investigating structures hidden inside or below transparent materials.

References

1. L. Loeber, O. Sutton, J. Morel, J.-M. Valletton, G. Muller, New direct observations of asphalts and asphalt binders by scanning electron microscopy and atomic force microscopy, *J. Microsc.* 182 (1) (1996) 32–39.
2. Loeber, G. Muller, J. Morel, O. Sutton, Bitumen in colloid science: a chemical, structural and rheological approach, *Fuel* 77 (13) (1998) 1443–1450.
3. A.T. Pauli, J.F. Branthaver, R.E. Robertson, W. Grimes, C.M. Eggleston, Atomic force microscopy investigation of SHRP asphalts, *ACS Div. Fuel Chem.* 46 (2) (2001) 104–110.
4. A. Jäger, R. Lackner, C. Eisenmenger-Sittner, R. Blab, Identification of four material phases in bitumen by atomic force microscopy, *Road Mater. Pavement Des.* 5 (2004) 9–24.
5. J.-F. Masson, V. Leblond, J. Margeson, Bitumen morphologies by phase detection atomic force microscopy, *J. Microsc.* 221 (1) (2006) 17–29.
6. H. Fischer, H. Stadler, N. Erina, Quantitative temperature-depending mapping of mechanical properties of bitumen at the nanoscale using the AFM operated with Peak Force Tapping TM mode: quantitative mapping of mechanics of bitumen, *J. Microsc.* 250 (3) (2013) 210–217.
7. H. Fischer, L.D. Poulikakos, J.-P. Planche, P. Das, J. Grenfell, Challenges while performing AFM on bitumen, in: N. Kringos, B. Birgisson, D. Frost, L. Wang (Eds.), *Multi-scale Modeling and Characterisation of Infrastructure Materials*, Springer, Dordrecht, the Netherlands, 2013, pp. 89–98.
8. S.N. Nahar, A.J.M. Schmets, A. Scarpas, G. Schitter, Temperature and thermal history dependence of the microstructure in bituminous materials, *Eur. Polym. J.* 48 (2013) 1964–1974, <https://doi.org/10.1016/j.eurpolymj.2013.03.027>.
9. T. Pauli, W. Grimes, A. Cookman, S.-C. Huang, Adherence energy of asphalt thin films measured by force-displacement atomic force microscopy, *J. Mater. Civ. Eng.* 26 (12) (2014) 04014089, [https://doi.org/10.1061/\(ASCE\)MT.1943-5533.0001003](https://doi.org/10.1061/(ASCE)MT.1943-5533.0001003).
10. H.R. Fischer, E.C. Dillingh, C.G.M. Hermse, On the microstructure of bituminous binders, *Road Mater. Pavement Des.* (2014) 1–15, <https://doi.org/10.1080/14680629.2013.837838>.
11. I. Menapace, E. Masad, A. Bhasin, D. Little, Microstructural properties of warm mix asphalt before and after laboratory-simulated long-term ageing, *Road Mater. Pavement Des.* 16 (suppl1.) (2015) 2–20, <https://doi.org/10.1080/14680629.2015.1029692>.
12. J. Blom, H. Soenen, A. Katsiki, N. Van den Brande, H. Rahier, and W. van den Bergh, Investigation of the bulk and surface microstructure of bitumen by atomic force microscopy. *Construction and Building Materials*, vol. 177, pp. 158-169, (2018).
13. H.R. Fischer, E.C. Dillingh, On the investigation of the bulk microstructure of bitumen – introducing two new techniques, *Fuel* 118 (2014), <https://doi.org/10.1016/j.fuel.2013.11.008>.
14. D. Ganter, S. Franzka, V. V. Shvartsman & D. C. Lupascu (2020) The phenomenon of bitumen 'bee' structures – bulk or surface layer – a closer look, *International Journal of Pavement Engineering*, DOI: 10.1080/10298436.2020.1823390
15. C. Xing, L. Liu, M. Li, Analysis of the nanoscale phase characteristics of bitumen and bitumen in mastics and mixtures via AFM First published: 04 June 2020 <https://doi.org/10.1111/jmi.12931>
16. P.K. Das, N. Kringos, V. Wallqvist, B. Birgisson, Micro-mechanical investigation of phase separation in bitumen by combining atomic force microscopy with differential scanning calorimetry results, *Road Mater. Pavement Des.* 14 (2013) 25–37, <https://doi.org/10.1080/14680629.2013.774744>.
17. H. Soenen, J. Besamusca, H.R. Fischer, L.D. Poulikakos, J.-P. Planche, P.K. Das, E. Chailleux, Laboratory investigation of bitumen based on round robin DSC and AFM tests, *Mater. Struct.* 47 (7) (2014), <https://doi.org/10.1617/s11527-013-0123-4>, pp. 1205–1220.
18. H. Soenen, P. Redelius, The effect of aromatic interactions on the elasticity of bituminous binders, *Rheol. Acta* 53 (9) (2014), <https://doi.org/10.1007/s00397-014-0792-0>, pp. 741–754
19. H.R. Fischer, Steven D. Mookhoek, A study of the influence of the microstructure of one type of bitumen grade on the performance as a binder, *Construction and Building Materials*, Volume 117, 2016, Pages 1-7, ISSN 0950-0618, <https://doi.org/10.1016/j.conbuildmat.2016.04.129>.
20. S. ds Santos, M.N. Partl, L.D. Poulikakos, Newly observed effects of water on the microstructures of bitumen surface ISSN: 0950–0618, *Constr. Build. Mater.* 71 (2014) 618–627, <https://doi.org/10.1016/j.conbuildmat.2014.08.076>.
21. A.M. Hung, A. Goodwin, E.H. Fini, Effects of water exposure on bitumen surface microstructure, *Constr. Build. Mater.* 135 (2017). 15 March 2017.
22. S. Bearsley, A. Forbes, R.G. Haverkamp, Direct observation of the asphaltene structure in paving-grade bitumen using confocal laser-scanning microscopy, *J. Microsc.* 215, (2004) 149–155.
23. X. Lu, M. Langtan, P. Olofsson, P. Redelius, Wax morphology in bitumen, *JOURNAL OF MATERIALS SCIENCE* 40 (2005) 1893 – 1900 (CLSM, polarised light microscopy (PLM))
24. H.R. Fischer, A. Cernescu, Relation of chemical composition to asphalt microstructure – Details and properties of micro-structures in bitumen as seen by thermal and friction force microscopy and by scanning near-field optical microscopy, *Fuel* 153 (2015) 628–633. OISSN: 016-2361.

25. A.Ramm, N. Sakib, A. Bhasin & M.C. Downer, Optical characterisation of temperature- and composition-dependent microstructure in asphalt binders, *Journal of Microscopy*, Vol. 00, Issue 0 2015, pp. 1–10 doi: 10.1111/jmi.12353
26. A. Ramm, M. C. Downer, N. Sakib and A. Bhasin, Morphology and kinetics of asphalt binder microstructure at gas, liquid, and solid interfaces, *J of microscopy* <https://onlinelibrary.wiley.com/doi/abs/10.1111/jmi.12842>
27. A. RAMM*, N. SAKIB†, A. BHASIN† & M.C. DOWNER , Correlated time-variation of bulk microstructure and rheology in asphalt binders, *Journal of Microscopy*, Vol. 271, Issue 3 2018, pp. 282–292 doi: 10.1111/jmi.12715
28. F. Handle, J. Füssl, S. Neudl, D. Grosseegger, L. Eberhardsteiner, B. Hofko, M. Hospodka, R. Blab, H. Grothe, *Materials and Structures* (2016) 49:167–180, DOI 10.1617/s11527-014-0484-3
29. Lu Xiaohu, P. Sjövall, H. Soenen, Structural and chemical analysis of bitumen using time-of-flight secondary ion mass spectrometry (TOF-SIMS), *Fuel* 199 (2017) 206–218. ISSN: 0016–2361.
30. X. Lu, M. Langton, P. Olofsson, P. Redelius, Wax morphology in bitumen, *JOURNAL OF MATERIALS SCIENCE* 40 (2005) 1893 – 1900
31. A.T. Pauli, R.W. Grimes, A.G. Beemer, T.F. Turner, J.F. Branthaver, Morphology of asphalts, asphalt fractions and model wax-doped asphalts studied by atomic force microscopy, *Int. J. Pavement Eng.* 12 (4) (2011) 291–309, <https://doi.org/10.1080/10298436.2011.575942>.
32. F. Pahlavan, M. Mousavi, A. Hung, E.H. Fini, Investigating molecular interactions and surface morphology of wax-doped asphaltenes, *J. Phys. Chem. Chem. Phys.* 18 (13) (2016) 8840–8854, <https://doi.org/10.1039/C5CP07180A>. The Royal Society of Chemistry.
33. Å.L. Lyne, V. Wallqvist, M.W. Rutland, P. Claesson, B. Birgisson, Surface wrinkling: the phenomenon causing bees in bitumen, *J. Mater. Sci.* 48 (20) (2013), <https://doi.org/10.1007/s10853-013-7505-4>, pp. 6970-6976.
34. Hung and E. Fini, AFM study of asphalt binder "bee" structures: origin, mechanical fracture, topological evolution, and experimental artifacts, *RSC Advances*, 2015), volume={5}, pages={96972-96982}
35. Minghui Gong, Jun Yang, Jianming Wei, Troy Pauli & Huayang Yu (2017) Quantitative characterisation of asphalt's composition–microstructure relationship based on atomic force microscopy, differential scanning calorimetry, and Fourier transform infrared spectroscopy tests, *Road Materials and Pavement Design*, 18:3, 507-532, DOI: 10.1080/14680629.2016.1181560
36. L. Zuzhong, F. Chunguang, Z. Hongyan, Z. Yayun, C. Huaxin, X. Haiwei, Investigation on evolution of bitumen composition and micro-structure during aging, *Construction and Building Materials*, Volume 244, 2020,118322,ISSN 0950-0618,<https://doi.org/10.1016/j.conbuildmat.2020.118322>.